

Studies on nanotribological and oxidation resistance properties of yttria stabilized zirconia (YSZ), alumina (Al₂O₃) based thin films developed by pulsed laser deposition

Nath, S, Manna, I, Ray, SK & Dutta Majumdar, J

Author post-print (accepted) deposited by Coventry University's Repository

Original citation & hyperlink:

Nath, S, Manna, I, Ray, SK & Dutta Majumdar, J 2016, 'Studies on nanotribological and oxidation resistance properties of yttria stabilized zirconia (YSZ), alumina (Al₂O₃) based thin films developed by pulsed laser deposition' *Ceramics International*, vol 42, no. 6, pp. 7060-7071

<https://dx.doi.org/10.1016/j.ceramint.2016.01.094>

DOI 10.1016/j.ceramint.2016.01.094

ISSN 0360-5442

ESSN 1873-6785

Publisher: Elsevier

NOTICE: this is the author's version of a work that was accepted for publication in *Ceramics International*. Changes resulting from the publishing process, such as peer review, editing, corrections, structural formatting, and other quality control mechanisms may not be reflected in this document. Changes may have been made to this work since it was submitted for publication. A definitive version was subsequently published in *Ceramics International*, [42, 6, (2017)] DOI: 10.1016/j.ceramint.2016.01.094

© 2017, Elsevier. Licensed under the Creative Commons Attribution-NonCommercial-NoDerivatives 4.0 International

<http://creativecommons.org/licenses/by-nc-nd/4.0/>

Copyright © and Moral Rights are retained by the author(s) and/ or other copyright owners. A copy can be downloaded for personal non-commercial research or study, without prior permission or charge. This item cannot be reproduced or quoted extensively from without first obtaining permission in writing from the copyright holder(s). The content must not be changed in any way or sold commercially in any format or medium without the formal permission of the copyright holders.

This document is the author's post-print version, incorporating any revisions agreed during the peer-review process. Some differences between the published version and this version may remain and you are advised to consult the published version if you wish to cite from it.

Studies on Nanotribological and Oxidation Resistance Properties of Yttria Stabilized Zirconia (YSZ) and Alumina (Al₂O₃) based Thin Films Developed by Pulsed Laser Deposition.

Subhasisa Nath^{a, 1}, Indranil Manna^{a, c, 2}, Samit Kumar Ray^{b, 3} and Jyotsna Dutta Majumdar^{a, 4, *}

^a *Department of Metallurgical & Materials Engineering, IIT, Kharagpur, West Bengal*

^b *Department of Physics, IIT, Kharagpur, West Bengal*

^c *Indian Institute of Technology, Kanpur*

¹sendsubha@gmail.com; ²imanna@metal.iitkgp.ernet.in;

³physkr@phy.iitkgp.ernet.in; ⁴jyotsna@metal.iitkgp.ernet.in

Abstract

The present study aims at evaluation of mechanical, tribological, and high temperature oxidation resistance (at 1000 °C under isothermal condition) properties of YSZ and Al₂O₃ thin films deposited by pulsed laser deposition technique. The mechanical and tribological properties of the YSZ and Al₂O₃ thin films showed significant improvement with increasing the deposition temperature during pulsed laser deposition process. However, the deposition temperature has no significant effect in reducing the TGO growth rate of the pulsed laser deposited YSZ and Al₂O₃ thin films as compared to that of conventional plasma sprayed thermal barrier coating.

Keywords: pulsed laser deposition, Young's modulus, hardness, tribology, oxidation

*Corresponding author, FAX: +91-3222-282280

1. Introduction

Yttria stabilized zirconia (YSZ) and aluminum oxide (Al_2O_3) are commonly used materials in aviation and power generation industries for heat, wear, and corrosion resistant applications due to its high melting point, low thermal conductivity, high hardness, chemical inertness, and thermo-mechanical compatibility with the underlying substrate [1- 3]. Oxidation of bond coat is the most detrimental phenomena responsible for failure of thermal barrier coated component as the formation and growth of thermally grown oxide (TGO) layer induces stress in the vicinity of TGO-top coat interface which increases with time and temperature of exposure [4, 5]. The oxidation of bond coat occurs by the diffusion of oxygen through the ceramic top coat followed by reaction with the elements present in the bond coat alloy. The diffusion of oxygen through the ceramic top coat proceeds by two mechanisms; (i) diffusion through the lattice by the movement of oxygen vacancies and (ii) gaseous movement through the interconnected pores and cracks present in the ceramic top coat [6]. The growth of TGO is mainly affected by the activity of oxygen at the bond coat and top coat interface. In the past, several investigations have been carried out to improve the oxidation resistance of TBC by designing the ceramic top coat [7-11]. Proving a functionally graded interlayer and dense top coat has been found to reduce the TGO growth rate significantly [7-11]. Deposition of materials with lower oxygen diffusivity has been beneficial in reducing the TGO growth rate and increasing the cyclic life of TBC [12-16]. Plasma sprayed Al_2O_3 /YSZ functionally graded TBC with an alumina interlayer showed an improved oxidation resistance as compared to conventional duplex TBC [17]. However, failure in Al_2O_3 /YSZ functionally graded TBC was observed due to development of significant residual stress as a result of presence of thick Al_2O_3 layer combined with phase transformation from γ -

Al_2O_3 to $\alpha\text{-Al}_2\text{O}_3$. Hence, deposition of a thin Al_2O_3 interlayer has been proposed instead of thick layer as thicker coating was found to induce more tensile residual stress in the coating.

Pulsed laser deposition (PLD) technique has been used as a preferred deposition technique for the development of Al_2O_3 and YSZ based thin films as compared to other physical vapor deposition technique due to the formation of near stoichiometric oxide [18-27]. The PLD technique involves irradiation of single or multiple targets by a focused pulsed-laser beam which results in melting, evaporation and ionization of species and formation of high density plasma plume made up of ablation species [18, 19]. However, the technique has not been extensively applied for the development and performance evaluation of oxide based thermal barrier coating.

In the present study, a detailed evaluation of the mechanical, tribological, and high temperature oxidation resistance (at 1000 °C under isothermal condition) properties of YSZ and Al_2O_3 based thin film deposited by pulsed laser deposition technique has been undertaken. The detailed investigation includes understanding the effect of substrate temperature on the microstructures and properties of YSZ and Al_2O_3 thin films. A detailed structure property correlation will be made to understand the role of microstructure on the properties of the thin film developed by pulsed laser deposition. Finally, the effect of thin film deposition on the high temperature oxidation behavior (under isothermal mode at 1000 °C) of plasma spray deposited YSZ based thermal barrier coating has been studied.

2. Experimental

2.1. Materials

7 wt% yttria stabilized zirconia (YSZ) powder (Amperit 831.007, 99.5% purity) and alumina (Al_2O_3) powder (Amperit 740.1, 99.95% purity) were chosen as starting materials for fabricating YSZ and Al_2O_3 pellets, respectively. The YSZ and Al_2O_3 precursor powders were cold pressed with an applied pressure of 10 ton followed by sintering in air at 1600 °C for 6 hours to fabricate pellets with diameter 25 mm. Different types of substrates were chosen for the deposition of thin films of YSZ and Al_2O_3 . Silicon wafer was used to deposit thin films for structural characterizations and nanoindentation test. For the evaluation of tribological behavior of the thin films, deposition of YSZ and Al_2O_3 films were carried out on predeposited CoNiCrAlY bond coat on Inconel 718 superalloy (dimension: 10 mm \times 10 mm \times 5 mm). The CoNiCrAlY bond coat with thickness 80 μm was deposited using high velocity oxy-fuel (HVOF) spray with process parameters reported elsewhere [10]. For the evaluation of high temperature oxidation, a conventional YSZ based duplex thermal barrier coating was chosen as substrate for deposition of thin films where YSZ top coat with thickness 300 μm was deposited by air plasma spraying on the surface of CoNiCrAlY bond coat with process parameters reported elsewhere [10]. Prior to pulsed laser deposition process, all the substrates were polished up to 0.05 μm surface finish followed by ultrasonically cleaned in soap solution followed by cleaning in acetone and ethyl alcohol.

2.2. Pulsed laser deposition

Fig. 1 shows the schematic representation of pulsed laser deposition process. Pulsed laser deposition of YSZ, Al_2O_3 , and Al_2O_3 /YSZ multilayered thin films were carried out using KrF

excimer laser system (Lambda Physik COMPEX, wavelength of 248 nm and pulsed duration of 25 ns). The cleaned substrates were mounted on a substrate holder inside the deposition chamber and placed parallel to the target which was mounted in a target holder at a perpendicular distance of 45 mm. The targets were continuously rotated to ensure uniform ablation and avoid pitting. The laser source was operated at a pulse repetition rate of 10 Hz and at an energy level of 300 mJ. For the deposition of monolithic film (only YSZ or Al_2O_3), 30000 laser shots were used. For the deposition of Al_2O_3 /YSZ multilayer film, Al_2O_3 was deposited first followed by YSZ. Alternative sequence of Al_2O_3 and YSZ (total 6 layers) was used for the deposition of multilayered thin film. For each layer, 5,000 laser shots were used so as to make a total of 30,000 laser shots equivalent to that of single layer deposition. The total time for deposition was 50 minutes. Films were deposited at substrate temperatures of 300 K, 573 K, 773 K, and 973 K. The deposition chamber was initially evacuated to 2.0×10^{-5} mbar and subsequently, filled with oxygen gas to a background pressure of 2×10^{-2} mbar.

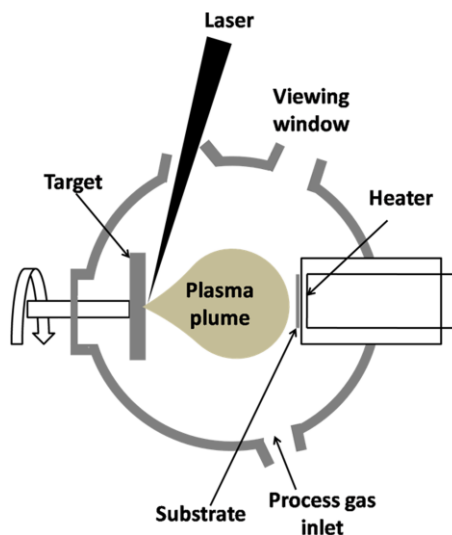


Fig. 1. Schematic representation of pulsed laser deposition process.

2.3. Characterization of thin films

Followed by pulsed laser deposition, a detailed observation of the microstructure of the as-deposited films was undertaken by field emission scanning electron microscopy (SUPRA 40, Zeiss SMT AG, Germany). A detailed analysis of the phase evolution was carried out by grazing incidence X-ray diffraction (GIXRD) technique (Bruker D8 Discover, Germany) with a grazing angle of 2° at a scanning speed of $0.05^\circ/\text{s}$. Cu $K\alpha$ radiation with wavelength 0.15418 nm was used as the X-ray source. The X-ray source was operated at an accelerating voltage of 40 kV and current of 40 mA. The diffraction angle was varied in the range of $20^\circ - 80^\circ$ with a scanning speed of $0.05^\circ/\text{s}$. The surface morphology and roughness of the deposited thin films were analyzed by atomic force microscopy (Agilent 5500 AFM, USA). The samples were scanned over an area of $5\ \mu\text{m} \times 5\ \mu\text{m}$ with a $90\ \mu\text{m}$ scanner at a scan rate of 1.5 line/s. The images were then exported to the Pico Image Basic 6.2 software for further analysis.

Residual stress developed on the surface of the coatings was measured by X-ray diffraction technique ($\sin^2\Psi$ technique) using a Bragg Brentano Diffractometer (Bruker D8 Discover, Germany). The X-ray source was operated at an accelerating voltage of 40 kV and current of 40 mA. The measurements of macrostresses in coatings were performed using Cu $K\alpha$ radiation with a step size of 0.05° and time per step of 5 s. In this method, $\theta/2\theta$ scans corresponding to a particular reflection or (hkl) were conducted at various tilt angles ψ (0, 15, 23, 45, 60) where ψ is the angle between the sample normal and the diffraction vector. For the calculation of residual stress, the (103) plane at $2\theta \approx 59^\circ$ of tetragonal zirconia phase was considered. For the calculation of residual stress, the (103) peak of tetragonal zirconia

phase was considered. The crystallite size and peak broadening analysis were performed using Scherrer's equation (for micro-stress) [28].

The biaxial residual stress was then calculated using Eq. (2.1).

$$\varepsilon_{\phi\psi} = \frac{d_{\phi\psi} - d_0}{d_0} = S_1^{hkl}(\sigma_{11} + \sigma_{22}) + \frac{1}{2} S_2^{hkl} \sigma_{\phi} \sin^2 \psi \quad (2.1)$$

where $d_{\phi\psi}$ is the interplanar spacing at a particular ϕ and ψ angle combination, d_0 is the strain free interplanar spacing, S_1^{hkl} and S_2^{hkl} are the X-ray elastic constants, σ_{ϕ} is the stress at ϕ direction and σ_{11} and σ_{22} are the principal stresses.

The hardness and Young's modulus of the deposited films were evaluated by nanoindentation test with a loading rate of 50 $\mu\text{N/s}$ up to a maximum load of 2000 μN (YSZ) and 500 μN (Al_2O_3) followed by holding at maximum load for 10 seconds and then unloading at a rate of 50 $\mu\text{N/s}$. The Oliver and Pharr method was used to measure the hardness and Young's modulus of the deposited films [29]. The nanotribological properties of the pulsed laser deposited YSZ and Al_2O_3 films were evaluated by Hysitron-TI950 Triboindenter with a Berkovich tip (tip radius < 150 nm) combined with a SPM. Nanoscratch test was used to measure the coefficient of friction of the deposited films by scratching the film surface with a constant force of 1 mN and 2 mN for Al_2O_3 and 4 mN and 5 mN for YSZ. A scratch velocity of 0.33 $\mu\text{m/s}$ was applied across a scratch length of 10 μm . The coefficient of friction of the films was measured by the ratio between the lateral force on the tip and the applied normal force. Adhesion strength of the films was measured by nanoscratch test under progressive loading from

0 mN to 350 mN at a loading rate of 11.7 mN/s and a scratch speed of 50 $\mu\text{m/s}$ covering a total scratch distance of 1000 μm (Al_2O_3) and 3000 μm (YSZ).

High temperature oxidation tests were conducted on conventional YSZ duplex TBC and pulsed laser deposited YSZ and Al_2O_3 thin films on plasma sprayed YSZ coating by holding the coated surface isothermally in static air at 1000 $^\circ\text{C}$ and subsequently, measuring the thickness of thermally grown oxide (TGO) layer at an interval of 24 hours up to a maximum of 96 hours. Thirty measurements were averaged out to calculate the TGO thickness. Followed by isothermal oxidation, a detailed observation of the microstructure and composition of the oxide scale was undertaken by scanning electron microscopy (SUPRA 40, Zeiss SMT AG, Germany) equipped with energy dispersive X-ray spectroscopy (EDS).

3. Results and Discussion

3.1. Characterization of the coating

Table 1 summarizes the characteristics of the YSZ, Al_2O_3 , and $\text{Al}_2\text{O}_3/\text{YSZ}$ multilayered thin films in terms of thickness, surface roughness (RMS value), microstructures and phase constituents, crystallite size, lattice strain and residual stress developed by pulsed laser deposition as a function of temperature of substrate. The thickness of the deposited films shows no specific trend with substrate temperature. The RMS roughness of YSZ thin film at 300 K, 573 K, 773 K, and 973 K are 12.9, 9.66 nm, 4.79 nm, and 4.28 nm, respectively. The maximum heights of the features present in the YSZ film deposited at 300 K, 573 K, 773 K, and 973 K are 220 nm, 90 nm, 45 nm, and 27 nm, respectively. The RMS roughness decreases with increase in substrate temperature (cf. Table 1) which is attributed to the decrease in particles height on the surface of YSZ film with increase in substrate temperature, T_s . The RMS roughness of Al_2O_3

films deposited at different substrate temperature is summarized in Table 1. The RMS roughness at 300 K, 573 K, 773 K, and 973 K are 7.31 nm, 3.3 nm, 2 nm, and 0.91 nm, respectively. The RMS roughness decreases with increase in substrate temperature (as shown in Table 1) which is attributed to the decrease in particles height on the surface of Al₂O₃ film with increase in substrate temperature, T_s. The maximum heights of the features present in the Al₂O₃ film deposited at 573 K, 773 K, and 973 K are 26 nm, 15 nm, and 13 nm, respectively.

Table 1
Summary of characteristics of the thin films deposited by PLD in the present study

Parameters	YSZ				Al ₂ O ₃				Al ₂ O ₃ /YSZ Multilayer
	300 K	573 K	773 K	973 K	300 K	573 K	773 K	973 K	300 K
Thickness, nm	2000 ± 60	141 ± 10	643 ± 90	1400 ± 20	391 ± 15	132 ± 10	157 ± 10	2336 ± 70	320 ± 10
Phases and its percentage	Amorphous	t-ZrO ₂ (~100%)	t-ZrO ₂ (~100%)	t-ZrO ₂ (~100%)	Amorphous	Amorphous	Amorphous	Amorphous	Amorphous
Crystallite size, nm	-	13	13	15	-	-	-	-	-
Lattice strain, %	-	0.77	0.75	0.69	-	-	-	-	-
Residual stress, GPa	-	-8.1 (σ_{11}) and -6.4 (σ_{22})	-7.5 (σ_{11}) and -5.5 (σ_{22})	-3.0 (σ_{11}) and -1.7 (σ_{22})	-	-	-	-	-
Roughness, nm	12.9	9.66	4.79	4.28	7.31	3.3	2	0.91	8.08

A detailed phase analysis shows that YSZ thin film deposited at room temperature is amorphous in nature. However, amorphous to crystalline structure transition occurs with increase in substrate temperature. At higher substrate temperature (≥ 573 K), single phase tetragonal zirconia (t-ZrO₂) phase is observed. On the other hand, the phase analysis of Al₂O₃ thin film shows amorphous nature of the film both at all the studied temperatures. The summary of variation of crystallite size, lattice strain, residual stress, and roughness of the thin films with substrate temperature is shown in Table 1. The average crystallite size in

YSZ thin film deposited at $T_s = 573$ K and 773 K shows similar value (13 nm). However, there is a marginal increase in crystallite size (15 nm) in the YSZ film deposited at $T_s = 973$ K. From Table 1, it may be noted that the lattice strain in YSZ films varies from 0.69% to 0.77%. The marginal decrease in lattice strain at higher substrate temperature may be attributed to stress relaxation due to higher mobility of adatoms due to increase in supply of thermal energy at higher substrate temperature [30]. The residual stress developed in YSZ thin films was measured by X-ray diffraction technique which is summarized in Table 1. From Table 1, it is evident that the residual stress in the deposited films decreases with increase in substrate temperature. The residual stress is predominantly compressive which is independent of substrate temperature. At $T_s = 573$ K, the residual stress component σ_{11} is -8.1 GPa which reduces to -3.0 GPa with increase in temperature (at $T_s = 973$ K). Similarly, the residual stress component σ_{22} is -6.4 GPa and at $T_s = 573$ K, which decreases to -1.7 GPa at 773 K. The higher residual compressive stress at low substrate temperature is attributed to the impingement of highly energetic species present in the plasma plume on to the substrate or on to the growing films and also due to thermal accommodation mismatch associated with the deposition at low temperature. The reduction in residual stress with increase in substrate temperature is attributed to the better surface diffusion of adatoms and gradual release of stress with increase in temperature [31, 32].

Fig. 2 shows the scanning electron micrographs of the top surface of as-deposited YSZ thin films at substrate temperature of (a) 300 K and (b) 973 K and as-deposited Al_2O_3 thin films at substrate temperature of (c) 300 K and (d) 973 K. Fig. 2 (a) reveals presence of a large number of particles or droplets on the surface of deposited YSZ films at 300 K. However, films deposited at 973 K shows a significantly reduced particle formation. From Fig. 2 (c), it is evident that

Al_2O_3 film deposited at 300 K contains particles or droplets, porosities and fine microcracks. On the other hand, thin film deposited at 973 K shows presence of lesser particles or droplets, porosities and microcracks (as shown by arrowheads). The formations of particles are commonly observed due to laser induced splashing of molten materials from the target and subsequent deposition along with the deposited film developed by ablation on the surface of substrate. The density of the molten particles and its dimension shows no specific trend with substrate temperature.

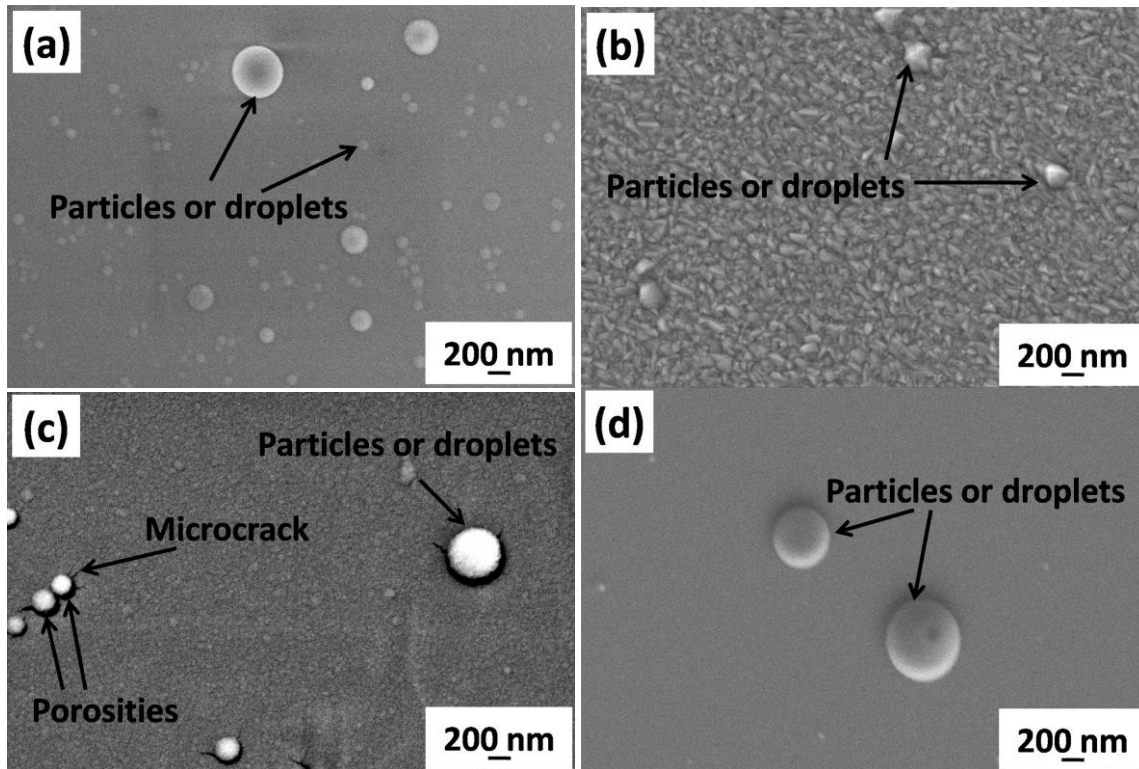


Fig. 2. Scanning electron micrographs of top surface of as-deposited YSZ thin films at (a) 300 K and (b) 973 K and as-deposited Al_2O_3 thin films (c) 300 K and (d) 973 K.

3.2. Nanomechanical properties

The nanomechanical properties of the YSZ and Al_2O_3 based thin films grown under different substrate temperature T_s were measured by nanoindentation technique. Fig. 3 shows the load-displacement curves of YSZ thin films grown under different substrate temperature, T_s . The variation of Young's modulus and hardness of YSZ thin films with different substrate temperatures is presented in Fig. 4. From Fig. 4, it may be noted that the Young's modulus of the YSZ thin films increases from 257 GPa at 300 K to 279 GPa at 973 K. However, an anomalous behavior in Young's modulus value of YSZ thin film is observed at 573 K. The increase in Young's modulus of the YSZ thin film with increase in deposition temperature is believed to be due to densification of microstructure (cf. Fig. 2). The reduced modulus (E_r) data reported for the YSZ thin film deposited at 300 K and 873 K were 257 GPa ($E_s = 271$ GPa) and 278 GPa ($E_s = 344$ GPa), respectively [23]. The Young's modulus value of plasma sprayed YSZ TBC in as-received condition was reported to be 155 GPa (at 8 mN load) [33]. The large difference in the Young's modulus of YSZ coating deposited by PLD method and APS method is due to the presence of significant amount microstructural defects (porosities and microcracks) in plasma sprayed YSZ TBC. The hardness value obtained at 300 K is found to be 13.7 GPa. The maximum value of hardness is found to be 23 GPa at 773 K. But exception in the trend occurred when the substrate temperature is raised to 973 K where, the hardness value decreases sharply to 16 GPa. The reported values of hardness for the amorphous and crystalline YSZ thin film deposited by PLD were 11.9 GPa and 16 GPa, respectively which are in good agreement with the results obtained in the present study [23]. Hardness of as-received YSZ TBC deposited by APS method was reported to be 9.9 GPa which is relatively small as compared to YSZ coating

deposited by PLD method [33]. The observed difference is due to the presence of microcracks and porosities in plasma sprayed YSZ coating.

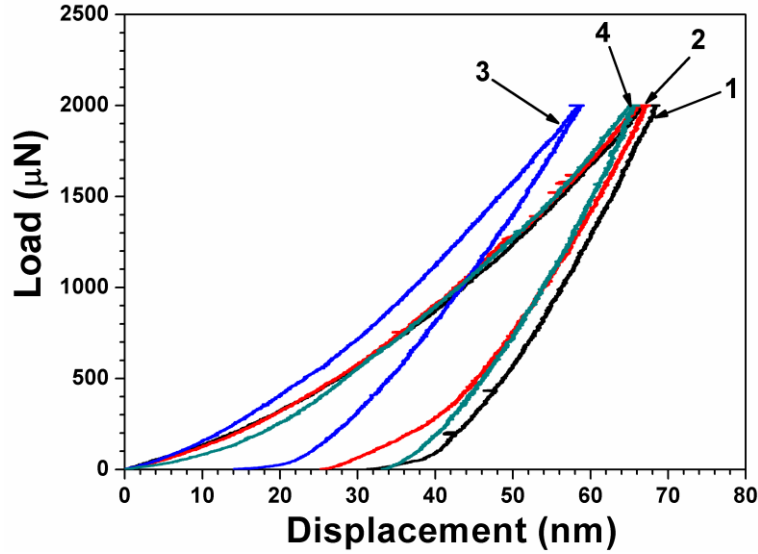


Fig. 3. Load versus displacement curve of as-deposited YSZ thin films at 300 K (plot 1), 573 K (plot 2), 773 K (plot 3), and 973 K (plot 4).

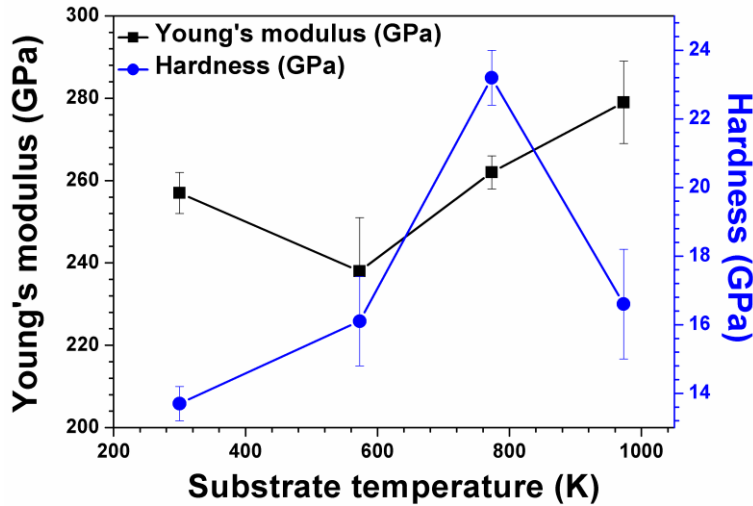


Fig. 4. Variation of Young's modulus and hardness in YSZ thin films with substrate temperature.

Fig. 5 shows the load-displacement curves for Al_2O_3 thin films grown under different substrate temperature (T_s). Fig. 6 shows the variation of Young's modulus and hardness in Al_2O_3 thin films with different substrate temperatures. From Fig. 6, it may be observed that the Young's modulus of the Al_2O_3 thin films increases from 94 GPa to 281 GPa with increase in substrate temperature (T_s) from 300 K to 973 K. Similarly, the hardness of deposited Al_2O_3 thin films increases from 3.3 GPa to 21.4 GPa. The increase in the Young's modulus and hardness of Al_2O_3 thin films with increase in substrate temperature is attributed to the densification of film with increase in substrate temperature. The hardness and Young's modulus of as-deposited amorphous Al_2O_3 thin film deposited by RF sputtering was reported to be 6 GPa and 116 GPa, respectively which are closely matching with the results obtained in the present study [34]. However, the reported hardness values of Al_2O_3 thin film (deposited by pulsed laser deposition) were 21 GPa and 25 GPa at 300 K and 973 K, respectively [26]. Similarly, the reported Young's modulus values of Al_2O_3 thin film (deposited by pulsed laser deposition) were 320 GPa and 360 GPa, when deposited by pulsed laser deposition at 300 K and 973 K, respectively [26].

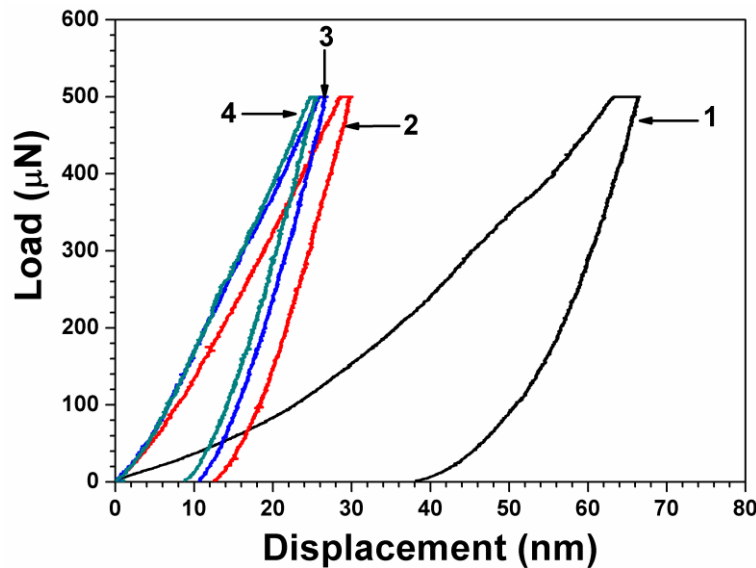


Fig. 5. Load versus displacement curve of as-deposited Al₂O₃ thin films at 300 K (plot 1), 573 K (plot 2), 773 K (plot 3), and 973 K (plot 4).

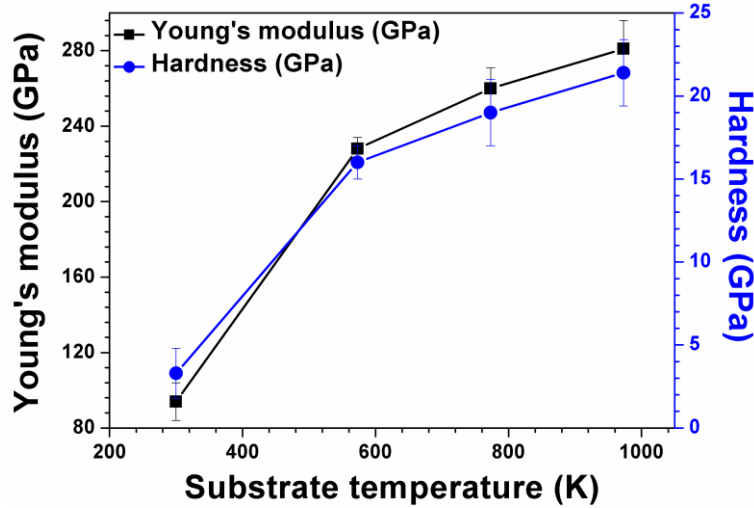


Fig. 6. Variation of Young's modulus and hardness in Al₂O₃ thin films with substrate temperature.

3.3. Coefficient of friction

Nanoscratch tests were performed on YSZ thin films grown at $T_s = 300$ K and 973 K under two different loads of 4 mN and 5 mN, respectively. The coefficient of friction (COF) was calculated by the ratio between the lateral force and normal force on the indenter. Fig. 7 shows the variation of COF with scratch length in YSZ thin films grown at 300 K (plot 1) and 973 K (plot 2) under the applied normal load of (a) 4 mN and (b) 5 mN. From Fig. 7, it is observed that the COF of YSZ thin films grown at room temperature shows a higher value as compared to that of the same grown at 973 K. It is also evident that the COF value of the YSZ thin film shows an abrupt change in friction value during scratch test, which may be attributed to sudden change in the lateral force value when the tip encounters with the microcracks and/or porosities present in the deposited YSZ thin films. Average COF of YSZ thin films under different applied loads and

temperature are shown in Table 2. From Table 2, it is evident that the average COF, at 4 mN applied load, shows a value of 0.406 and 0.344 for the films deposited at 300 K and 973 K, respectively. Similarly, the average COF, at 5 mN applied load, shows a value of 0.403 and 0.328 for the films deposited at 300 K and 973 K, respectively. Hence, it may be concluded that the COF value decreases with increase in substrate temperature. The decrease in coefficient of friction value with increase in substrate temperature is attributed to the decrease in surface roughness with increase in substrate temperature.

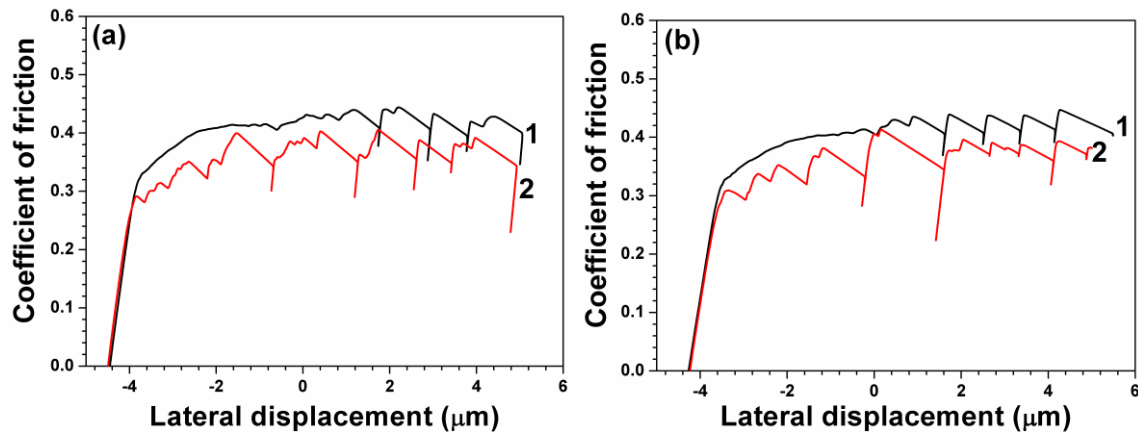


Fig. 7. Variation of coefficient of friction (COF) with scratch length in YSZ thin films grown at 300 K (plot1) and 973 K (plot 2) under applied load of (a) 4 mN and (b) 5 mN.

Table 2

Average COF in YSZ thin films deposited by pulsed laser deposition grown at 300 K and 973 K.

4 mN		5 mN	
300 K	973 K	300 K	973 K
0.406	0.344	0.403	0.328

Fig. 8 shows the variation of COF with scratch length in Al_2O_3 thin films grown at 300 K (plot 1) and 973 K (plot 2) under the applied normal load of (a) 1 mN and (b) 2 mN. From Fig. 8 (a, b), it is observed that the COF of Al_2O_3 thin films grown at room temperature shows a higher value as compared to that of the same grown at 973 K. It is also evident that COF curves of Al_2O_3 thin films shows sharp fluctuations during scratch test which may be attributed to sudden change in the lateral force value when the tip encounters with the microcracks and/or porosities present in the Al_2O_3 thin films. Average COF values of Al_2O_3 thin films under different applied loads and temperature are shown in Table 3. From Table 3, it is evident that the average COF under 1 mN applied load shows a COF value of 0.406 and 0.344 for the films deposited at 300 K and 973 K, respectively. Similarly, the average COF under 2 mN applied load shows a value of 0.403 and 0.328 for the films deposited at 300 K and 973 K, respectively. Hence, it can be concluded that the COF value decreases with increase in substrate temperature for Al_2O_3 thin films due to decrease in surface roughness with increase in substrate temperature. The increase in hardness at higher deposition temperature is another reason for decreasing COF value as higher hardness leads to formation of lesser debris.

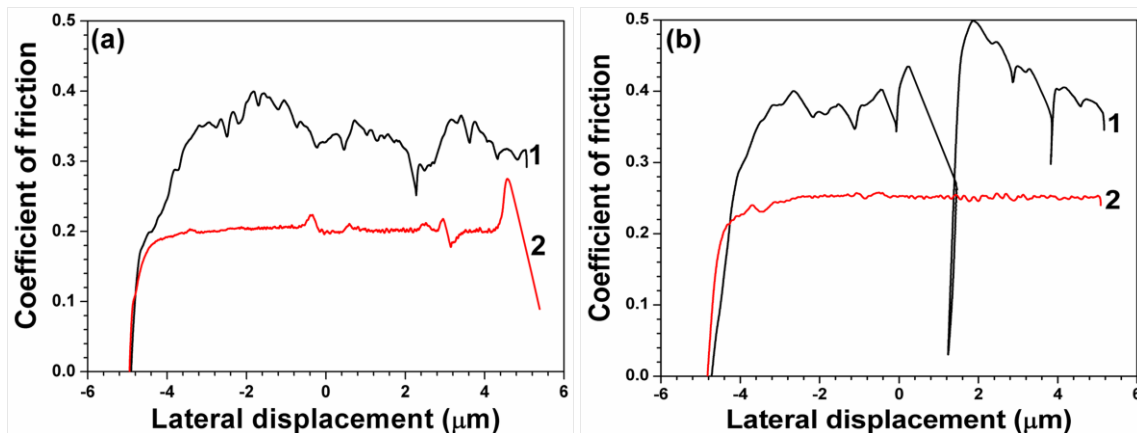


Fig. 8. Variation of coefficient of friction (COF) with time in Al₂O₃ thin films grown under 300 K (plot 1) and 973 K (plot 2) under the applied normal load of (a) 1 mN and (b) 2 mN.

Table 3

Average COF in Al₂O₃ thin films deposited by pulsed laser deposition grown at 300 K and 973 K.

1mN		2 mN	
300 K	973 K	300 K	973 K
0.337	0.204	0.332	0.251

3.4. Adhesion strength

Nanoscratch tests were carried out to measure the adhesion strength under scratching [35]. During the scratching, shear stress is progressively developed at the substrate-film interface. When the developed shear stress reaches its critical value (i.e. higher than interfacial adhesion strength), the film starts to delaminate. The delaminated films come under the scratch tip during scratching which results in the stress development and release which leads to the fluctuation in the curves. The adhesion strength of the thin film can be measured as the load at which there is a fluctuation in the applied normal load versus scratch length curve during scratching under ramp mode. Fig. 9 shows the variation of applied normal force (curve 1) and lateral force (curve 2) with the scratch length in YSZ thin films grown at (a) 300 K and (b) 973 K. The critical applied normal load in which film spallation occurs is represented as L_c . From Fig. 9 (a), it may be noted that the critical applied normal load (L_c) at which the film delamination occurs is 141 mN for YSZ film developed at 300 K. The lateral force curve, as shown in Fig. 9 (a), shows localized fluctuations, initially, up to certain scratch distance, beyond which it changes to a continuous

fluctuation. On the other hand, the critical load (L_c) at which the YSZ film deposited at 973 K started rupturing is 278 mN as shown in Fig. 9 (b). The initial localized sharp increase of lateral force, in the curve is attributed to (1) interaction of scratch tip with the particles present on the surface of YSZ thin films which results in generation of a high lateral force due to the hindrance faced by the indenter during scratching and (2) localized deformation of the YSZ film (as shown by arrowheads in Fig. 9 (b)) resulting due to poor adhesion of the film with the substrate because of the presence of underlying defects. Beyond the critical load, the lateral force shows periodical fluctuations which is attributed to the interaction of scratch tip with the delaminated YSZ films during which stress development and release occurs. Comparison of Fig. 9 (a) with Fig. 9 (b), it may be inferred that the critical load (L_c) for delamination or in other words, the adhesion strength of the YSZ film deposited at higher substrate temperature (i.e. $T_s = 973$ K) is higher than that of the same deposited at room temperature (i.e. $T_s = 300$ K). The improvement in adhesion strength of the YSZ film deposited at 973 K as compared to the film deposited at 300 K is attributed to the increase in the bonding between the film and the substrate due to interdiffusion of atoms from YSZ and CoNiCrAlY at higher substrate temperature [36, 37]. The improvement in the adhesion strength of YSZ thin film deposited at 973 K may also be attributed to the reduction in thermal stress due to development of Al_2O_3 thermal grown oxide (TGO) layer at the interface of bond coat and YSZ film as the difference in thermal expansion coefficient between YSZ and Al_2O_3 is small as compared to the difference in thermal expansion coefficient between YSZ and CoNiCrAlY metallic bond coat. A close comparison between Fig. 9 (a) and Fig. 9 (b) also shows that there is less fluctuation of the lateral force during scratch testing on the coating deposited at a substrate temperature of 973 K as compared to the film deposited at 300 K which

can be corroborated with the top surface microstructure of the YSZ thin film deposited at 300 K and 973 K which suggests that density of particle formation decreases with increase in substrate temperature.

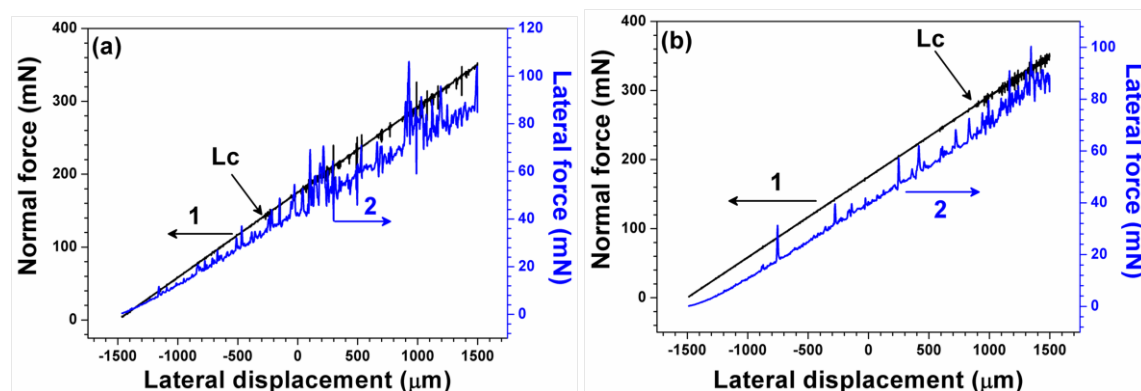


Fig. 9. Variation of applied normal force (plot 1) and lateral force (plot 2) with scratch length in YSZ thin films grown at (a) 300 K and (b) 973 K.

Fig. 10 shows the scanning electron micrographs of nanoscratch track of YSZ thin film grown at (a) 300 K and (b) 973 K. From Fig. 10 (a), it can be seen that the YSZ film grown at 300 K is delaminated after attaining the critical load for complete spallation of film. A wedge type spallation is observed in YSZ film grown at 300 K. Localized plastic deformations are observed during nanoscratch in the film before the critical load for complete spallation of the film as shown by arrowheads in Fig. 10 (b). A wedge type spallation is also observed for YSZ film grown at 973 K. Comparison of Fig. 10 (a) with Fig. 10 (b) reveals that the failure of YSZ film grown at 300 K started at an earlier stage as compared to the YSZ film grown at 973 K. In addition, the width of the spalled region of YSZ film grown at 300 K is found to be larger as compared to the YSZ film grown at 973 K. Hence, it may be concluded that the YSZ film grown at 973 K shows improved adhesion as compared to YSZ film grown at 300 K.

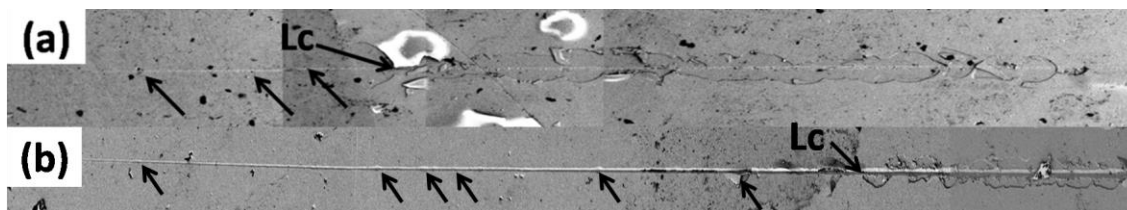


Fig. 10. Scanning electron micrographs of nanoscratch track of YSZ thin films grown at (a) 300 K and (b) 973 K.

Fig. 11 shows the variation of applied normal force (curve 1) and lateral force (curve 2) with the scratch length in Al_2O_3 thin films grown at (a) 300 K and (b) 973 K, respectively. From Fig. 11 (a), it may be noted that the lateral force curve shows continuous fluctuation whereas, the normal force curve shows no evidence of fluctuation. In addition, there is no sudden change in normal force or lateral force values in the curve. From Fig. 11 (b), it may also be observed that the lateral force and normal force shows no signature of abrupt change in the curve. The fluctuations in the lateral force curve are due to presence of obstructions (particles and underlying defects) on the surface of the film which requires a higher lateral force to move further. However, a relatively less fluctuations in the lateral force curve may be observed as compared to the Al_2O_3 film deposited at 300 K which is possibly due to decrease in density of particles formed on the surface of Al_2O_3 film deposited at 973 K.

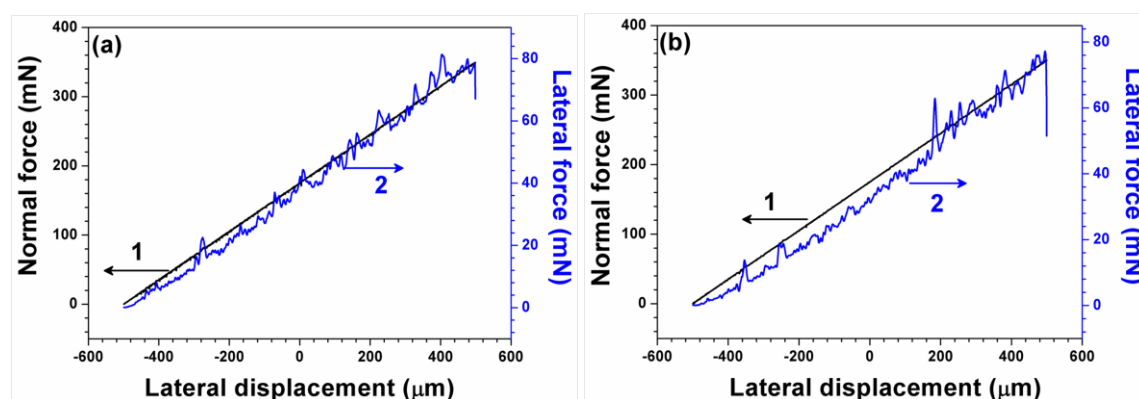


Fig. 11. Variation of applied normal force (plot 1) and lateral force (plot 2) with scratch length in Al_2O_3 thin films grown at (a) 300 K and (b) 973 K.

Fig. 12 shows the scanning electron micrographs of nanoscratch track of Al_2O_3 thin film grown at (a) 300 K and (b) 973 K. Fig. 12 (a) shows severe plastic deformation of the Al_2O_3 thin films deposited at 300 K in the onset of scratching which continues till the end of nanoscratch process. The failure of the film may be attributed to (a) development of stress due to large difference in coefficient of thermal expansion (CTE) between the Al_2O_3 film ($\text{CTE} = 6.65 \times 10^{-6} \text{ K}^{-1}$ [38]) and CoNiCrAlY coating ($\text{CTE} = 13.22 \times 10^{-6} \text{ K}^{-1}$ [38]) and (b) very low hardness of the Al_2O_3 film deposited at 300 K (cf. Fig. 3). The large fluctuations in the lateral force curve accounts for presence of debris on the wear track (cf. Fig. 12 (a)). On the other hand, the Al_2O_3 thin film deposited at 973 K shows superior adhesion strength up to the applied normal load of 350 mN. The improved adhesion strength of the Al_2O_3 thin film deposited at 973 K may be attributed to the improvement in chemical bonding between the substrate and Al_2O_3 thin film due to interdiffusion of atoms from Al_2O_3 and CoNiCrAlY [36, 37]. Formation of Al_2O_3 scale due to oxidation of aluminum present in CoNiCrAlY coating is thought to be another possible reason in improving the adhesion strength of the film as the difference in thermal expansion coefficient reduces, significantly. Enhanced hardness of the Al_2O_3 thin films deposited at 973 K may also have significant contribution in improving the adhesion strength of the film.

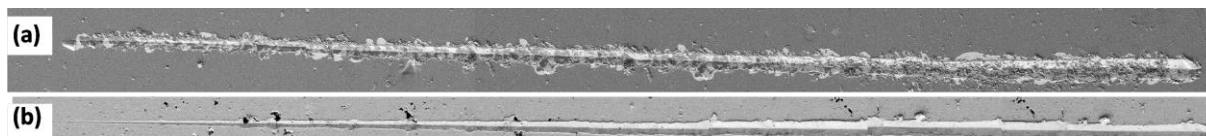


Fig. 12. Scanning electron micrographs of nanoscratch track of Al_2O_3 thin films grown at (a) 300 K and (b) 973 K.

From the investigation, it is observed that the thin film deposited at higher substrate temperature shows significant improvement in mechanical and tribological properties. But, the high temperature deposition for TBC application is not advisable as thermally grown oxide layer may develop on the surface of CoNiCrAlY bond or at the interface between CoNiCrAlY bond coat and YSZ top coat due to oxidation of aluminum present in the bond coat alloy. The oxidation of aluminium would decrease the concentration of aluminium in the bond coat alloy below its critical value to maintain a stable alumina growth. The compositional change in the bond coat alloy will also change the TGO chemistry during high temperature exposure. Hence, a room temperature deposition is suggested for the thin film deposition on plasma sprayed TBC.

3.5. High temperature oxidation

High temperature oxidation tests were carried out for thin films deposited on plasma sprayed YSZ deposited at 300 K. Although thin films deposited at 973 K shows improved properties, films deposited at 300 K were only chosen for high temperature oxidation due to the fact that with higher substrate temperature the CoNiCrAlY surface is prone to develop Al_2O_3 scale during thin film deposition process which decreases the concentration of aluminum in the CoNiCrAlY required during high temperature exposure. Fig. 13 shows the variation of TGO thickness with time in conventional duplex TBC (plot 1), pulsed laser deposited YSZ thin film (plot 2), Al_2O_3 thin film (plot 3), and Al_2O_3 /YSZ multilayer thin film (plot 4) on plasma sprayed YSZ during isothermal oxidation at 1000 °C up to 96 hour. From Fig. 13, it can be observed that the TGO growth kinetics shows parabolic nature. From Fig. 13, it may be seen that during initial stage of oxidation the growth kinetics is faster up to 24 hour of oxidation which then slows down till 96 hour of oxidation. The fast oxidation kinetics at initial stage may be attributed to the migration of

oxygen through the film and coating followed by its reaction with aluminum present in the bond coat alloy to form Al_2O_3 . As soon as a stable Al_2O_3 forms at the interface between top coat and bond coat, it retards oxygen to diffuse through it and thereby, reducing the oxidation kinetics. From plot 1 and plot 2, it may be noted that there is no significant difference in TGO thickness in conventional duplex TBC and the pulsed laser deposited YSZ thin film which is attributed to the fact that the YSZ film is not effective in reducing the rate of oxygen diffusion due to the fact that YSZ is a good oxygen ion conductor. On the other hand, marginal reduction in TGO growth rate is observed for Al_2O_3 thin film (plot 3) and Al_2O_3 /YSZ multilayer thin film (plot 4) as Al_2O_3 has the lowest oxygen diffusivity [39]. The small difference in TGO thickness of conventional duplex TBC (plot 1) and the pulsed laser deposited Al_2O_3 thin film (plot 3) and Al_2O_3 /YSZ multilayer thin film (plot 4) at initial stage of oxidation may be attributed to the presence of inter-columnar porosities in pulsed laser deposited films at 300 K which acts as an active path for oxygen diffusion. However, with increase in time of isothermal exposure at 1000 °C, the films started to sinter as a result of grain growth as observed in Fig. 13. The closure of porosities reduces the rate of oxygen diffusion through the film and as a result of which a decrease in oxygen activity occurs at the bond coat and top coat interface. The decrease in oxygen activity helps to slow down the TGO growth rate in pulsed laser deposited Al_2O_3 thin film and Al_2O_3 /YSZ multilayer thin film.

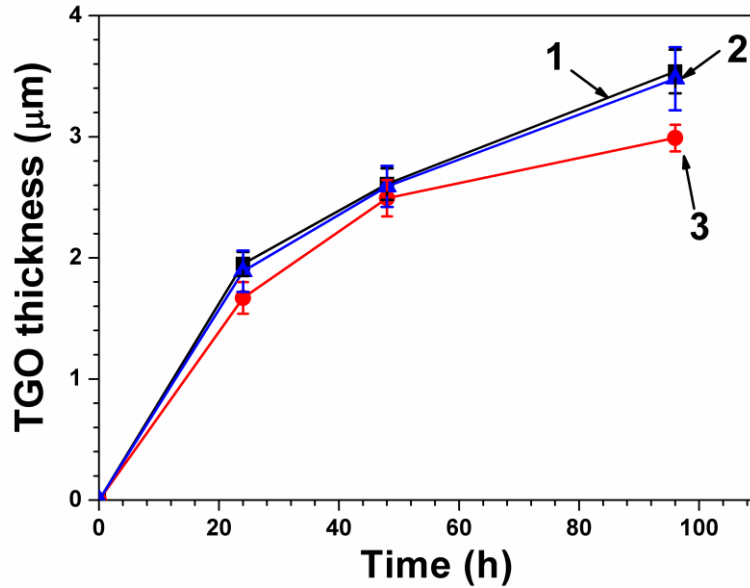


Fig. 13. Variation of TGO thickness with time for conventional CoNiCrAlY/YSZ duplex TBC (plot 1), pulsed laser deposited YSZ thin film on plasma sprayed YSZ (plot 2), pulsed laser deposited Al_2O_3 thin film on plasma sprayed YSZ (plot 3), and pulsed laser deposited Al_2O_3 /YSZ multilayer thin film on plasma sprayed YSZ (plot 4) after isothermal oxidation at 1000 °C for 96 hours.

Fig. 14 shows the scanning electron micrograph of top surface of pulsed laser deposited YSZ thin film, Al_2O_3 thin film, and Al_2O_3 /YSZ multilayer thin film on plasma sprayed YSZ after isothermal oxidation at 1000 °C up to 96 hour. From Fig. 14 (a) the grain growth is evident. Equiaxed grains of size ranging from ~ 300 nm to 1.5 μm are observed on the surface of oxidized pulsed laser deposited YSZ thin film. From Fig. 14 (b), it may be noted that the surface of pulsed laser deposited Al_2O_3 thin film shows dense film, however few cracks are also found on its surface. The presence of cracks in pulsed laser deposited Al_2O_3 thin film may be due to the underlying surface defects present on the surface of plasma sprayed YSZ coating. From Fig. 14 (c), it can also be observed that equiaxed grains of size ranging from ~ 300 nm to 1.5 μm are also present on the surface of oxidized pulsed laser deposited Al_2O_3 /YSZ thin film. Few cracks are

also found on the surface of YSZ thin film and $\text{Al}_2\text{O}_3/\text{YSZ}$ multilayer thin film as a result of underlying defect present on the surface of plasma sprayed YSZ coating.

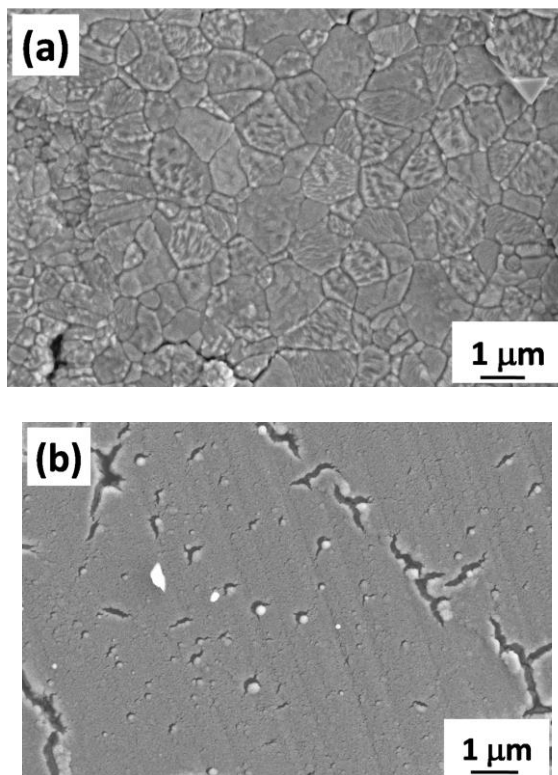


Fig. 14. Scanning electron micrographs of top surface isothermally oxidized pulsed laser deposited (a) YSZ, (b) Al_2O_3 , and (c) $\text{Al}_2\text{O}_3/\text{YSZ}$ multilayer films on plasma sprayed YSZ TBC at 1000 °C for 96 h.

Fig. 15 shows the scanning electron micrograph of cross-section of oxidized (a) plasma sprayed duplex TBC and pulsed laser deposited (b) YSZ thin film, (b) Al_2O_3 thin film, (c) $\text{Al}_2\text{O}_3/\text{YSZ}$ multilayer thin film on plasma sprayed YSZ TBC at 1000 °C for 96 hour. From Fig. 15, it can be seen that a thermally grown oxide (TGO) layer is formed at the interface between metallic CoNiCrAlY bond coat and ceramic YSZ top coat in a continuous manner. A TGO layer forms due to reaction of elements present in the CoNiCrAlY bond coat, preferentially aluminum, with oxygen diffused through the thin film and/or coating layer at elevated temperature. During oxidation, oxygen initially diffuses through the interconnected porosities and microcracks

present in the film and coating and by lattice diffusion and thereby oxidizing the bond coat forming TGO at the bond coat and top coat interface. As soon as a stable oxide layer forms on the surface of bond coat, the rate of oxidation reduces. From Fig. 15, it is evident that the TGO consisted of a dark grey oxide layer is found to be Al_2O_3 (with composition of 36.02-38.37 at. % Al and 61.62-63.98 at. % O as determined by EDS analysis). CoNiCrAlY bond coat contains ~ 8 wt% of aluminum which upon exposure to high temperature oxidizing environment forms various oxides of Al_2O_3 on top of bond coat.

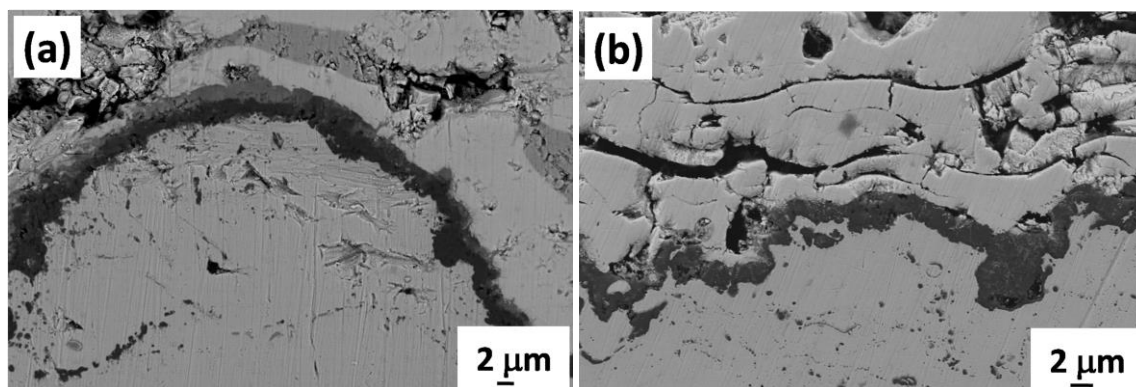


Fig. 15. Scanning electron micrographs of cross-section isothermally oxidized (a) plasma sprayed YSZ duplex TBC and pulsed laser deposited (b) YSZ, (c) Al_2O_3 , (d) $\text{Al}_2\text{O}_3/\text{YSZ}$ multilayer films on plasma sprayed YSZ TBC at 1000 °C up to 96 h.

4. Summary & Conclusions

In the present study, the mechanical, tribological, and high temperature oxidation behavior of pulsed laser deposited yttria stabilized zirconia and alumina thin films has been studied in detail.

From the detailed investigations, the following conclusions may be drawn:

1. The mechanical properties (hardness and Young' modulus) of the YSZ and Al_2O_3 thin films were found to increase with increase in substrate temperature. Young's modulus of YSZ thin films was found to vary between 237 GPa and 278 GPa at the studied substrate

temperatures. Similarly, hardness of the YSZ thin film varies between 14 GPa and 23 GPa. On the other hand, the Young's modulus of Al_2O_3 thin film at room temperature was found to be 94 GPa which increased to 280 GPa at 973 K. Similarly, hardness was increased from 3 GPa at 300 K to 23 GPa at 973 K.

2. Tribological property of the PLD grown YSZ and Al_2O_3 films were improved significantly upon increasing the substrate temperature. COF of YSZ thin films grown at room temperature showed a higher value (0.406 and 0.403 at 4 mN and 5 mN, respectively) as compared to that of same grown at 973 K (0.344 and 0.328 at 4 mN and 5 mN, respectively). COF of Al_2O_3 grown at 300 K showed higher value (0.337 and 0.332 at 1 mN and 2 mN, respectively) as compared to the same grown at 973 K (0.204 and 0.251 at 1 mN and 2 mN, respectively).

3. Adhesion strength measured by nanoscratch testing showed a superior bond strength of YSZ films deposited at 973 K (critical load for delamination (L_c): 278 mN) than film deposited at 300 K (critical load for delamination (L_c): 141 mN).

4. In case of Al_2O_3 thin film deposited at 300 K, a severe plastic deformation was observed at the initial stage of scratching which continued till the end of the test. On the other hand, Al_2O_3 film deposited at 973 K showed improved in adhesion strength by not showing any signature of delamination up to the 350 mN of applied normal load.

5. The high temperature oxidation behavior of Al_2O_3 thin film and Al_2O_3 /YSZ multilayer thin film on plasma sprayed YSZ at 1000 °C showed marginal improvement in oxidation resistance over conventional duplex TBC.

Acknowledgement

The partial financial support from the Department of Science and Technology (DST), New Delhi, Council of Scientific and Industrial Research, New Delhi and Indian Space Research Organization (ISRO) are gratefully acknowledged.

References

- [1] R.A. Miller, Thermal barrier coatings for aircraft engines: history and directions, *J. Therm. Spray Technol.* 6 (1997) 35–42.
- [2] J.F. Li, H. Liao, X.Y. Wang, B. Normand, V. Ji, C.X. Ding, C. Coddet, Improvement in wear resistance of plasma sprayed yttria stabilized zirconia coating using nanostructured powder, *Tribol. Int.* 37 (2004) 77–84.
- [3] A. G. Evans, D. R. Mumm, J. W. Hutchinson, G. H. Meier, F. S. Pettit, Mechanisms controlling the durability of thermal barrier coatings, *Prog. Mater Sci.* 46 (2001) 505–553.
- [4] W. R Chen, X. Wu, B. R. Marple, P. C. Patnaik, Oxidation and crack nucleation/growth in an air-plasma-sprayed thermal barrier coating with NiCrAlY bond coat, *Surf. Coat. Technol.* 197 (2005) 109–115.
- [5] E.A.G. Shillington, D.R. Clarke, Spalling failure of a thermal barrier coating associated with aluminum depletion in the bond-coat, *Acta Mater.* 47 (1999) 1297–1305.
- [6] A.C. Fox, T.W. Clyne, Oxygen transport by gas permeation through the zirconia layer in plasma sprayed thermal barrier coatings, *Surf. Coat. Technol.* 184 (2004) 311–321.
- [7] S. Nath, I. Manna, J. Dutta Majumdar, Compositionally graded thermal barrier coating by hybrid thermal spraying route and its non-isothermal oxidation behavior, *J. Therm. Spray Technol.* 22 (2013) 901–917.
- [8] S. Nath, I. Manna, J. Dutta Majumdar, Kinetics and mechanism of isothermal oxidation of compositionally graded yttria stabilized zirconia (YSZ) based thermal barrier coating, *Corros. Sci.* 88 (2014) 10–22.

- [9] K.A. Khor, Y.W. Zu, Thermal properties of plasma-sprayed functionally graded thermal barrier coatings, *Thin Solid Films* 372 (2000) 104–113.
- [10] Y.N. Wu, F.H. Wang, W.G. Hua, J. Gong, C. Sun, L.S. Wen, Oxidation behavior of thermal barrier coatings obtained by detonation spraying, *Surf. Coat. Technol.* 166 (2003) 189–194.
- [11] J. H. Park, J. S. Kim, K. H. Lee, Y. S. Song, M. C. Kang, Effects of the laser treatment and thermal oxidation behavior of CoNiCrAlY/ZrO₂–8wt%Y₂O₃ thermal barrier coating, *J. Mater. Process. Technol.* 201 (2008) 331–335.
- [12] J. H. Sun, E. Chang, C. H. Chao, M. J. Cheng, The spalling modes and degradation mechanism of ZrO₂-8 wt.% Y₂O₃/CVD-Al₂O₃/Ni-22Cr-10Al-1Y thermal barrier coatings, *Oxid. Met.* 40 (1993) 465–481.
- [13] S. Widjaja, A. M. Limarga, T. H. Yip, Oxidation behavior of a plasma-sprayed functionally graded ZrO₂/Al₂O₃ thermal barrier coating, *Mater. Lett.* 57 (2002) 628–634.
- [14] Y.-F. Su, L.F. Allard, D.W. Coffey, W.Y. Lee, Effects of an α -Al₂O₃ Thin film on the oxidation behavior of a single-crystal Ni-based superalloy, *Metall. Mater. Trans. A* 35 (2004) 1055–1065.
- [15] Y. J. Su, R. W. Trice, K. T. Faber, H. Wang, W. D. Porter, Thermal conductivity, phase stability, and oxidation resistance of Y₃Al₅O₁₂ (YAG)/Y₂O₃–ZrO₂ (YSZ) thermal barrier coatings, *Oxid. Met.* 61 (2004) 253–271.
- [16] C. R. C. Lima, N. Cinca, J. M. Guilemany, Study of the high temperature oxidation performance of thermal barrier coatings with HVOF sprayed bond coat and incorporating a PVD ceramic interlayer, *Ceram. Int.* 38 (2012) 6423–6429.
- [17] A. M. Limarga, S. Widjaja, T. H. Yip, Mechanical properties and oxidation resistance of plasma-sprayed multilayered Al₂O₃/ZrO₂ thermal barrier coatings, *Surf. Coat. Technol.* 197 (2005) 93–102.
- [18] X. Zhang, W. Ren, P. Shi, A. Tian, H. Xin, X. Chen, X. Wu, X. Yao, Influence of substrate temperature on structures and dielectric properties of pyrochlore Bi_{1.5}Zn_{1.0}Nb_{1.5}O₇ thin films prepared by pulsed laser deposition, *Appl. Surf. Sci.* 256 (2010) 6607–6611.
- [19] C. R. Cho, A. Grishin, Self-assembling ferroelectric Na_{0.5}K_{0.5}NbO₃ thin films by pulsed-laser deposition, *Appl. Phys. Lett.* 75 (1999) 268–270.

- [20] J. Y. Paek, I. Chang, J. H. Park, S. Ji, S. W. Cha, A study on properties of yttrium-stabilized zirconia thin films fabricated by different deposition techniques, *Renewable Energy* 65 (2014) 202-206.
- [21] G. Balakrishnan, T. N. Sairam, V.R. Reddy, P. Kuppusami, Jung Il Song, Microstructure and optical properties of $\text{Al}_2\text{O}_3/\text{ZrO}_2$ nano multilayer thin films prepared by pulsed laser deposition, *Mater. Chem. Phys.* 140 (2013) 60-65.
- [22] S. Heiroth, R. Frison, J. L.M. Rupp, T. Lippert, E. J. B. Meier, E. M. Gubler, M. Döbeli, K. Conder, A. Wokaun, L. J. Gauckler, Crystallization and grain growth characteristics of yttria-stabilized zirconia thin films grown by pulsed laser deposition, *Solid State Ionics* 191 (2011) 12–23.
- [23] S. Heiroth, R. Ghisleni, T. Lippert, J. Michler, A. Wokaun, Optical and mechanical properties of amorphous and crystalline yttria-stabilized zirconia thin films prepared by pulsed laser deposition, *Acta Mater.* 59 (2011) 2330–2340.
- [24] H. Hidalgo, E. Reguzina, E. Millon, A. L. Thomann, J. Mathias, C. Boulmer-Leborgne, T. Sauvage, P. Brault, Yttria-stabilized zirconia thin films deposited by pulsed-laser deposition and magnetron sputtering, *Surf. Coat. Technol.* 205 (2011) 4495–4499.
- [25] J. Shin, P. Li, J. Mazumder, Pulsed laser deposition of the yttria-stabilized zirconia films, *Thin Solid Films* 517 (2008) 648–651.
- [26] G. Balakrishnan, S. Tripura Sundari, R. Ramaseshan, R. Thirumurugesan, E. Mohandas, D. Sastikumar, P. Kuppusami, T. G. Kim, J. I. Song, Effect of substrate temperature on microstructure and optical properties of nanocrystalline alumina thin films, *Ceram. Int.* 39 (2013) 9017–902.
- [27] G. Balakrishnan, P. Kuppusami, S. Tripura Sundari, R. Thirumurugesan, V. Ganesan, E. Mohandas, D. Sastikumar, Structural and optical properties of γ -alumina thin films prepared by pulsed laser deposition, *Thin Solid Films* 518 (2010) 3898–3902.
- [28] B. D. Cullity, *Elements of X-ray Diffraction*, second ed., Addison-Wesley, Menlo Park, CA, 1956.
- [29] W. C. Oliver, G. M. Pharr, An improved technique for determining hardness and elastic modulus sing load and displacement sensing indentation experiments, *J. Mater. Res.* Vol. 7 (1992) 1564-1583.
- [30] G. Balakrishnan, P. Sudhakara, Abdul Wasy, Ha Sun Ho, K.S. Shin, J.I. Song, Epitaxial growth of cerium oxide thin films by pulsed laser deposition, *Thin Solid Films* 546 (2013) 467–471.

- [31] M. Tabbal, S. Kahwaji, T.C. Christidis, B. Nsouli, K. Zahraman, Pulsed laser deposition of nanostructured dichromium trioxide thin films, *Thin Solid Films* 515 (2006) 1976–1984.
- [32] J. Xiong, W. Qin, X. Cui, B. Tao, J. Tang, Y. Li, Effect of processing conditions and methods on residual stress in CeO₂ buffer layers and YBCO superconducting films, *Physica C* 442 (2006) 124–128.
- [33] S. Nath, I. Manna, J. Dutta Majumdar, Nanomechanical behavior of yttria stabilized zirconia (YSZ) based thermal barrier coating, *Ceram. Int.* 41 (2015) 5247–5256.
- [34] I. Neelakanta Reddy, V. Rajagopal Reddy, N. Sridhara, V. Sasidhara Rao, Manjima Bhattacharya, Payel Bandyopadhyay, S. Basavaraja, Anoop Kumar Mukhopadhyay, Anand Kumar Sharma, Arjun Dey, Pulsed rf magnetron sputtered alumina thin films, *Ceram. Int.* 40 (2014) 9571–9582.
- [35] H. C. Barshilia, B. Deepthi, G. Srinivas, K. S. Rajam, Sputter deposited low-friction and tough Cr-Si₃N₄ nanocomposite coatings on plasma nitrided M2 steel, *Vacuum* 86 (2012) 1118–1125.
- [36] S.Y. Chang, Y.C. Hsiao, Y.C. Huang, Preparation and mechanical properties of aluminum-doped zinc oxide transparent conducting films, *Surf. Coat. Technol.* 202 (2008) 5416–5420.
- [37] B. Rahmati, A.A.D. Sarhan, Z. Kamiab, E. Zalnezhad, B. Nasiri, W.A.B.W. Abas, Enhancing the adhesion strength of tantalum oxide ceramic thin film coating on biomedical Ti-6Al-4V alloy by thermal surface treatment, *Ceram. Int.* <http://dx.doi.org/10.1016/j.ceramint.2015.07.090>.
- [38] C. Nordhorn, R. Mücke, K. A. Unocic, M. J. Lance, B. A. Pint, R. Vaßen, Effects of thermal cycling parameters on residual stresses in alumina scales of CoNiCrAlY and NiCoCrAlY bond coats, *Surf. Coat. Technol.* 258 (2014) 608–614.
- [39] W.Y. Lee, D.P. Stinton, C.C. Berndt, F. Erdogan, Y.D. Lee, Z. Mutasim, Concept of functionally graded materials for advanced thermal barrier coating applications: A review, *J. Am. Ceram. Soc.* 79 (1996) 3003–3012.

CITATION

S. Nath, I. Manna, S.K. Ray, J. Dutta Majumdar, Studies on nanotribological and oxidation resistance properties of yttria stabilized zirconia (YSZ) and alumina (Al₂O₃) based thin films developed by pulsed laser deposition, *Ceramics International* 42 (2016) 7060–7071. doi.org/10.1016/j.ceramint.2016.01.094.

